Focusing and imaging using eigenfunctions of the scattering operator

T. Douglas Mast[a)]
Department of Electrical Engineering, University of Rochester, Rochester, New York 14642

Adrian I. Nachman
Department of Mathematics, University of Rochester, Rochester, New York 14627

Robert C. Waag
Departments of Electrical Engineering and Radiology, University of Rochester, Rochester, New York 14627

(Received 15 October 1996; accepted 14 February 1997)

An inverse scattering method that uses eigenfunctions of the scattering operator is presented. This approach provides a unified framework that encompasses eigenfunction methods of focusing and quantitative image reconstruction in arbitrary media. Scattered acoustic fields are described using a compact, normal operator. The eigenfunctions of this operator are shown to correspond to the far-field patterns of source distributions that are directly proportional to the position-dependent contrast of a scattering object. Conversely, the eigenfunctions of the scattering operator specify incident-wave patterns that focus on these effective source distributions. These focusing properties are employed in a new inverse scattering method that represents unknown scattering media using products of numerically calculated fields of eigenfunctions. A regularized solution to the nonlinear inverse scattering problem is shown to result from combinations of these products, so that the products comprise a natural basis for efficient and accurate reconstructions of unknown inhomogeneities. The corresponding linearized problem is solved analytically, resulting in a simple formula for the low-pass-filtered scattering potential. The linear formula is analytically equivalent to known filtered-backpropagation formulas for Born inversion, and, at least in the case of small scattering objects, has advantages of computational simplicity and efficiency. A similarly efficient and simple formula is derived for the nonlinear problem in which the total acoustic pressure can be determined based on an estimate of the medium. Computational results illustrate focusing of eigenfunctions on discrete and distributed scattering media, quantitative imaging of inhomogeneous media using products of retransmitted eigenfunctions, inverse scattering in an inhomogeneous background medium, and reconstructions for data corrupted by noise. [S0001-4966(97)02308-4]

PACS numbers: 43.20.Fn, 43.60.Pt, 43.35.Wa, 43.80.Qf [ANN]

INTRODUCTION

This paper presents a new inverse scattering method that employs the focusing properties of certain acoustic fields obtained by retransmitting eigenfunctions of the scattering operator.

Eigensystem decomposition of the scattering operator, regardless of the inversion method employed, has potential advantages in methods of collecting and analyzing scattering data. Previous work in electrical impedance tomography has employed eigenfunction decomposition of an operator associated with the measurement process to determine optimal input current patterns and quantify the achievable resolution of imaging systems.[1,2] These optimal inputs can also be determined by iteratively retransmitting input patterns that are proportional to the measured scattered field. This approach is essentially an analog implementation of the ''power method'' for determining the eigenvectors of matrices.[2,3]

Likewise, the techniques of optical and acoustic phase conjugation[4–7] and the analogous process of time reversal[8,9] can be understood as analog methods of computing the eigenfunctions of an operator associated with the phase conjugation or time-reversal process. Simple focusing by phase conjugation, in which received echoes are conjugated or time reversed and retransmitted, is equivalent to a single iteration of the power method. Further iterations of this procedure correspond to additional steps in the power method, and thus converge to the most significant eigenfunction of the associated operator at a rate specified by the ratio of the two largest eigenvalues.[3] The eigenfunctions of the ''time-reversal operator,'' whether obtained by iterative time reversal or by numerical diagonalization, have been previously shown to correspond to source distributions that can focus incident energy on strong, pointlike scatterers.[10,11]

Eigensystem analysis has historically played a role in the theory of inverse scattering for radially symmetric objects.[12] For these objects, separation of variables naturally leads to a representation of the scattering operator in terms of trigonometric functions. Since these eigenfunctions are the same for any radial scatterer, the inverse scattering problem could be reduced to the problem of determining the unknown object from the eigenvalues of the scattering operator.

[a)]Current affiliation: Applied Research Laboratory, The Pennsylvania State University, P.O.B. 30, State College, PA 16802.

However, before the method presented here, the focusing properties of eigenfunctions have not been exploited for quantitative reconstruction of inhomogeneous media. It is stated in Ref. 9 that the concept of time reversal ''cannot be directly compared to computed tomography'' or to ''techniques that generate the image of the medium through signal analysis.'' Although the basic principles of focusing on point targets using the eigenfunctions of scattering operators have been put forth in Ref. 10, these principles have not previously been shown to apply to general distributed inhomogeneities. Furthermore, no general imaging method has hitherto been based on these principles.

The current method presents a solution to the imaging problem by bringing together recent results in the theory of focusing, diffraction tomography, and inverse problems to synthesize a unified framework for quantitative imaging of inhomogeneous media. Application of the method shows that focusing on distributed inhomogeneities can be achieved using eigenfunctions and also provides a technique for quantitative imaging of discrete and distributed inhomogeneities using focusing properties.

This method has several advantages over current inverse scattering methods. First, the eigenfunction formulation provides optimal bases for reconstruction of unknown media, so that inversions are performed with the minimum possible complexity. Second, the method is applicable to any scattering medium for which the total acoustic pressure associated with an incident plane wave can be estimated. Inverse scattering in inhomogeneous background media as well as iterative nonlinear inverse scattering can therefore be directly implemented. Third, part of the computation necessary for the inverse scattering algorithm can be performed by analog means using ideas from the power method.

The present approach also provides new understanding about existing methods of focusing and imaging. For simple scattering objects, the new method presented here reduces to a quantitative specification of focusing similar to that obtained by iterative phase conjugation or time reversal. The eigenfunctions of scattering operators are shown not only to focus on pointlike scatterers, as has been previously shown,[10,11] but also to concentrate incident energy in the vicinity of general, distributed inhomogeneities. The method also improves on previous approaches to focusing using eigenfunctions in that quantitative images of medium parameters are obtained simultaneously with optimal incident-wave distributions. For the case of weakly scattering objects, the method reduces to a simple inversion algorithm that is mathematically equivalent to the filtered backpropagation algorithm,[13–15] but is optimally tailored to the unknown scattering medium. The method reduces to a comparably simple and efficient formula for the case of weakly nonlinear inverse scattering.

Analysis given in Sec. I shows that eigenfunctions of scattering operators are equal to the acoustic fields of effective source distributions that are proportional to the compressibility contrast of the scattering object. An inverse scattering method that incorporates products of retransmitted fields of eigenfunctions is presented. The general method is then employed to derive an analytic inversion formula valid under the Born approximation as well as a simple nonlinear formula valid for small multiple-scattering effects. Numerical implementation of these methods is presented in Sec. II. Numerical results shown in Sec. III illustrate focusing on discrete and distributed inhomogeneities using a few eigenfunctions. Also, quantitative inverse scattering results are shown both within the context of a homogeneous background medium and an inhomogeneous background medium.

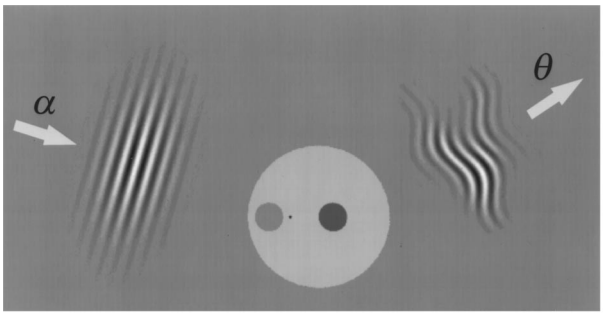

FIG. 1. Scattering configuration. An incident plane wave traveling in the direction $\boldsymbol{\alpha}$ is scattered by an inhomogeneity and the scattered field is measured in the direction $\boldsymbol{\theta}$.

I. THEORY

A. Background

An inverse scattering method for a medium of variable sound speed is derived. For simplicity of exposition, the derivation is given for the canonical two-dimensional scattering configuration sketched in Fig. 1. However, with minor modifications, the method is applicable to arbitrary geometries and dimensions.

When the incident pressure is a plane wave of unit amplitude propagating in the direction $\boldsymbol{\alpha}$, so that $p_i(\mathbf{x})=e^{ik\boldsymbol{\alpha}\cdot\mathbf{x}}$, the corresponding total acoustic pressure $p(\mathbf{x},\alpha)$ at the position $\mathbf{x}$ is given by the Lippman–Schwinger equation[16,17]

$$p(\mathbf{x},\alpha)=e^{ik\boldsymbol{\alpha}\cdot\mathbf{x}}-\int G_0(\mathbf{x}-\mathbf{y},k)q(\mathbf{y})p(\mathbf{y},\alpha)dy, \qquad (1)$$

where $G_0(\mathbf{x}-\mathbf{y})$ is the Green's function for the Helmholtz equation in a homogeneous medium. In an unbounded two-dimensional medium, $G_0(\mathbf{x}-\mathbf{y})$ is given by the Hankel function $(i/4)H_0^{(1)}(k|\mathbf{x}-\mathbf{y}|)$.[18] The angle α is defined as the angle corresponding to the direction unit vector $\boldsymbol{\alpha}$, the wave number k is equal to $2\pi f/c_0$ where c_0 is the wave speed of the background medium, and f is the temporal frequency of the incident wave. The integral appearing in Eq. (1), as well as subsequent integrals in x and y, are understood to be taken over the entire plane in $\mathbb{R}^2$. The scattering potential q is given for a medium of variable sound speed by

$$q(\mathbf{x})=-k^2\left(\frac{c_0^2}{c^2(\mathbf{x})}-1\right). \qquad (2)$$

The quantity within parentheses is equal, for a medium of constant density, to the compressibility contrast γ_κ, as defined in Ref. 17. The scattering potential is assumed to be

real-valued and to be short-range, that is, the potential q decreases at large distances such that

$$|q(\mathbf{x})| \leq C(1+|\mathbf{x}|)^{-1-\delta}, \tag{3}$$

where $|\mathbf{x}|$ is the magnitude of the position vector $\mathbf{x}$, for some $\delta > 0$.

At a measurement radius r in the far field and a measurement angle θ, the scattered pressure, $p_s = p - p_i$, is of the form

$$p_s(r,\theta,\alpha) = -\sqrt{\frac{i}{8\pi}}\,\frac{e^{ikr}}{\sqrt{kr}} A(\theta,\alpha) + o\left(\frac{1}{\sqrt{kr}}\right), \tag{4}$$

where A is the far-field pattern of the scattered pressure

$$A(\theta,\alpha) = \int e^{-ik\boldsymbol{\theta}\cdot\mathbf{x}} q(\mathbf{x}) p(\mathbf{x},\alpha)\, dx. \tag{5}$$

The incident pressure may be more generally taken as a superposition of plane waves propagating in all directions,

$$p_i(\mathbf{x}) = \int f(\alpha) e^{ik\boldsymbol{\alpha}\cdot\mathbf{x}}\, d\alpha. \tag{6}$$

The far-field pattern of the corresponding scattered acoustic pressure is then

$$Af(\theta) = \int A(\theta,\alpha) f(\alpha)\, d\alpha. \tag{7}$$

Equation (7) defines an operator A that maps an incident-wave distribution $f(\theta)$ into the corresponding far-field scattered pressure $Af(\theta)$. The operator A is related to the usual scattering operator S (Ref. 19) by

$$S = I - \frac{i}{4\pi} A, \tag{8}$$

where I is the identity operator.

The operator A is compact[19] and therefore has a countable number of discrete eigenvalues with zero as the only possible cluster point. In practice, only a finite number of eigenvalues are distinguishable from zero. Since the potential q is real-valued, the scattering operator is unitary, so that the eigenvalues of A lie in the complex plane on the circle centered at $-4\pi i$ and passing through the origin. It also follows that A is normal ($A^*A = AA^*$, where A^* is the Hermitian transpose of A), so that an orthonormal basis $\{f_i\}$ for $L^2[0,2\pi]$ exists consisting of eigenfunctions of A.

Since A is a normal operator, the Hermitian transpose A^* satisfies the relation $A^* f_i = \lambda^* f_i$, where f_i is an eigenfunction of A and λ_i^* is the complex conjugate of λ_i. The eigenfunctions of A therefore also satisfy the equation

$$A^*A f_i = |\lambda_i|^2 f_i. \tag{9}$$

Thus the functions f_i also constitute a basis of eigenfunctions for A^*A and the corresponding eigenvalues are the squared magnitudes of the eigenvalues of A. The operator A^*A is essentially a far-field analog of the ''time-reversal operator'' as defined in Ref. 10.

B. Focusing properties

The focusing properties of A are seen by considering the ratio of the scattered amplitude to the incident amplitude. Since A is normal, the magnitude of its largest eigenvalue is equal to the largest possible value of this ratio for any nonzero f:

$$|\lambda_1| = \sup\left[\frac{\|Af(\theta)\|_{L^2}}{\|f(\theta)\|_{L^2}}\right], \tag{10}$$

where $\sup(\cdot)$ denotes the least upper bound and $\|f(\cdot)\|_{L^2}$ denotes the root-mean-square magnitude of a square-integrable function. Thus the eigenfunction associated with the largest eigenvalue of A specifies an incident-wave distribution that maximizes the energy scattered to the far field. Other eigenfunctions also focus energy on inhomogeneities with an efficiency that is quantified by the associated eigenvalues.

The focusing property of eigenfunctions of A is further illustrated by introducing the acoustic fields of incident-wave distributions specified by the eigenfunctions. One may define retransmitted fields of an incident-wave distribution $f(\alpha)$ as

$$\begin{aligned} E(\mathbf{x}) &= \int f(\alpha) e^{ik\boldsymbol{\alpha}\cdot\mathbf{x}}\, d\alpha, \\ F(\mathbf{x}) &= \int f(\alpha) p(\mathbf{x},\alpha)\, d\alpha, \end{aligned} \tag{11}$$

where $E(\mathbf{x})$ is the retransmitted field associated with the incident-wave distribution in a homogeneous medium and $F(\mathbf{x})$ is the retransmitted field in a medium containing the inhomogeneity $q(\mathbf{x})$.

For incident-wave patterns corresponding to eigenfunctions that have nonzero eigenvalues, the retransmitted fields of Eqs. (11) can be written using Eqs. (5) and (7) in the form

$$\begin{aligned} E_i(\mathbf{x}) &= \frac{2\pi}{\lambda_i} \int J_0(k|\mathbf{x}-\mathbf{y}|) F_i(\mathbf{y}) q(\mathbf{y})\, dy, \\ F_i(\mathbf{x}) &= \frac{1}{\lambda_i} \int \langle p(\mathbf{x},\theta), e^{ik\boldsymbol{\theta}\cdot\mathbf{y}} \rangle F_i(\mathbf{y}) q(\mathbf{y})\, dy. \end{aligned} \tag{12}$$

The brackets in Eq. (12) denote the inner product

$$\langle u, v \rangle = \int_0^{2\pi} u(\theta) v^*(\theta)\, d\theta, \tag{13}$$

while the inner product appearing in the expression for E_i was evaluated using the identity

$$J_0(z) = \frac{1}{2\pi} \int e^{iz\cos\theta}\, d\theta \tag{14}$$

known as Parseval's integral.[20] The retransmitted fields of Eq. (11) are thus seen to be equivalent to a weighted convolution of the unknown scattering potential with inner products of acoustic fields.

When the scattering potential $q(\mathbf{x})$ is concentrated in a finite number of pointlike scatterers, each very small compared to a wavelength, Eq. (12) reduces to an expression of diffraction-limited focusing on each point scatterer. That is, for a scattering medium defined by

$$q(\mathbf{x})=\sum_{1}^{M}\mu_j\delta(\mathbf{x}-\mathbf{x_j}), \tag{15}$$

the retransmitted field $E_i(\mathbf{x})$ is

$$E_i(\mathbf{x})=\frac{2\pi}{\lambda_i}\sum_j F_i(\mathbf{x}_j)J_0(k|\mathbf{x}-\mathbf{x_j}|)\mu_j, \tag{16}$$

so that in this case, the retransmitted field $E_i(\mathbf{x})$ is equal to a weighted sum of Bessel functions, each centered at the location of one of the point scatterers. These Bessel functions correspond to a group of diffraction-limited main lobes, centered at each scatterer position $\mathbf{x_j}$, with corresponding Bessel sidelobes that combine coherently. Thus each retransmitted field E_i focuses to some extent on all of the individual point scatterers.

The close relationship between the retransmitted fields of eigenfunctions and the unknown scattering potential, as seen in Eq. (12), is an expression of the focusing property of eigenfunctions. That is, since eigenfunctions of A correspond to incident-wave patterns that concentrate energy within the support of the scattering potential, they can be said to focus on general distributed inhomogeneities as well as pointlike scatterers. This idea is illustrated numerically later in this paper.

C. Inverse scattering method

Because of the focusing properties outlined above, retransmitted fields of eigenfunctions are a useful starting point for inverse scattering reconstructions. A general inverse scattering method incorporating these ideas is outlined below.

The starting point for this method is an expression of the inverse scattering problem in terms of the operator A of Eq. (7) and the corresponding retransmitted fields defined in Eq. (11):

$$\langle Af_i,f_j\rangle=\delta_{ij}\lambda_i=\int F_i(\mathbf{x})E_j^*(\mathbf{x})q(\mathbf{x})dx, \quad i,j=1,2,\ldots . \tag{17}$$

The problem can be regularized by seeking the solution that minimizes the weighted L^2 norm

$$\|q\|_W^2=\int |q(\mathbf{x})|^2W(\mathbf{x})dx \tag{18}$$

with $W(\mathbf{x})$ an appropriate weight. For the analysis given below, this weight is defined as $W(\mathbf{x})=(1+|\mathbf{x}|)^{\delta},\delta>0$. For the explicit computations given later, other choices of $W(\mathbf{x})$ are more natural.

A solution to the minimization problem is obtained using the method of Lagrange multipliers, analogous to the approach used in Ref. 21 for a linearized electric impedance tomography problem. At a minimum, the (infinite-dimensional) gradient of $\|q\|_W^2$ is a linear combination of the gradients of the constraints in Eq. (17). The latter can be calculated using the two-potential formula[16]

$$A_{q_1}(\theta,\alpha)-A_{q_2}(\theta,\alpha)=\int p_1(\mathbf{x},\alpha)\times(q_1(\mathbf{x})-q_2(\mathbf{x}))p_2(\mathbf{x},\theta+\pi)dx, \tag{19}$$

where A_{q_1}, p_1, A_{q_2}, and p_2 are the scattering operators and the total acoustic pressures for the inhomogeneous media defined by $q_1(\mathbf{x})$ and $q_2(\mathbf{x})$, respectively. Equation (19) yields the derivative

$$\lim_{\epsilon\to 0}\frac{A_{q+\epsilon\tilde{q}}(\theta,\alpha)-A_q(\theta,\alpha)}{\epsilon}=\int p(\mathbf{x},\alpha)\tilde{q}(\mathbf{x})p(\mathbf{x},\theta+\pi)dx, \tag{20}$$

while the infinite-dimensional gradient of $\|q\|_W^2$ is found from

$$\lim_{\epsilon\to 0}\frac{\|q+\epsilon\tilde{q}\|_W^2-\|q\|_W^2}{\epsilon}=2\int q(\mathbf{x})\tilde{q}(\mathbf{x})W(\mathbf{x})dx. \tag{21}$$

The result follows that if the potential $q_M(\mathbf{x})$ solves the regularized inverse scattering problem [minimization of the weighted norm from Eq. (18) under the constraint of Eq. (17)], q_M must be of the form

$$q_M(\mathbf{x})=\frac{1}{W(\mathbf{x})}\sum_l\sum_m Q_{lm}F_l(\mathbf{x})\overline{F_m^*}(\mathbf{x}), \tag{22}$$

where $\overline{F_m^*}(\mathbf{x})$, the complex conjugate of the retransmitted field corresponding to an incoming condition at infinity, is defined as

$$\overline{F^*}(\mathbf{x})=\int f^*(\alpha)p(\mathbf{x},\alpha+\pi)d\alpha, \tag{23}$$

and the coefficients Q_{lm} are the Lagrange multipliers. If the above gradients are taken with respect to the real and imaginary parts of a complex potential, Eq. (22) as stated is also found to be valid when the potential q_M is complex. In some of the simplifying approximations made below, Eq. (22) will yield a complex potential q_M even when the data are assumed to come from a unitary scattering operator associated with the real potential q.

By substituting Eq. (22) into Eq. (17), the inverse problem is reduced to the problem of finding the coefficients Q_{lm} from the nonlinear system

$$\delta_{ij}\lambda_i=\sum_l\sum_m\left[\int\frac{F_i(\mathbf{x})E_j^*(\mathbf{x})F_l(\mathbf{x})\overline{F_m^*}(\mathbf{x})}{W(\mathbf{x})}dx\right]Q_{lm}, \quad i,j=1,2,\ldots , \tag{24}$$

where the dependence of the fields F and $\overline{F^*}$ on the scattering potential q is implicit.

In general, the scattering potential $q(\mathbf{x})$, and therefore the total pressure field $p(\mathbf{x},\alpha)$, are unknown in inverse scattering problems. The function $p(\mathbf{x},\alpha)$ that implicitly appears in Eq. (24) may therefore be replaced by the best available estimate for the total pressure. Equation (24) can then be solved for the coefficients Q_{lm} by standard numerical techniques for solution of linear systems.

The number of terms N can be chosen arbitrarily; however, increasing N beyond the number of nonzero eigenval-

ues of A is of limited benefit in reconstructions. For simple scattering objects, q can be represented by expansions employing small values of N. For instance, for an inhomogeneity consisting of finitely many point scatterers, N comparable to the number of scatterers is sufficient.

The above method simplifies further in the case of a weakly scattering medium, for which the total pressure p can be approximated by the incident pressure. In this case, taking the weight $W(\mathbf{x})\equiv 1$, the coefficients Q_{lm} can be evaluated analytically. From Eq. (22), under the Born approximation, the scattering potential takes the form

$$q_B(\mathbf{x})=\sum_l \sum_m Q_{lm}E_l(\mathbf{x})E_m^*(\mathbf{x}). \tag{25}$$

Substituting Eq. (25) into Eq. (5) gives the equation

$$A(\theta,\alpha)=\sum_l \sum_m Q_{lm}\int e^{-ik\boldsymbol{\theta}\cdot\mathbf{x}}E_l(\mathbf{x})E_m^*(\mathbf{x})p(x,\alpha)dx. \tag{26}$$

Replacement of $p(\mathbf{x},\alpha)$ in Eq. (26) by the incident plane wave $e^{ik\boldsymbol{\alpha}\cdot\mathbf{x}}$, use of Eq. (11), and integration in $\mathbf{x}$ over $\mathbb{R}^2$ yields

$$A(\theta,\alpha)=\frac{(2\pi)^2}{k^2}\sum_l \sum_m Q_{lm}\int_{-\pi}^{\pi}\int_{-\pi}^{\pi}\delta(\boldsymbol{\theta}-\boldsymbol{\alpha}-\boldsymbol{\theta}'+\boldsymbol{\alpha}') \times f_l(\theta')f_m^*(\alpha')d\theta'\,d\alpha' \tag{27}$$

for $\theta-\alpha$ not equal to 0 or π. The double integral in Eq. (27) can be evaluated using the change of variables

$$x_1'=\cos\,\theta'-\cos\,\alpha', \quad x_2'=\sin\,\theta'-\sin\,\alpha', \tag{28}$$

which is one-to-one when restricted to the regions $\alpha'<\theta'$ and $\alpha'>\theta'$. Evaluation of the integral yields

$$|\sin(\theta-\alpha)|A(\theta,\alpha)=\frac{(2\pi)^2}{k^2}\sum_l \sum_m Q_{lm}(f_l(\theta)f_m^*(\alpha) + f_l(\alpha+\pi)f_m^*(\theta+\pi)). \tag{29}$$

Equation (29) can be solved for the coefficients Q_{lm} using the fact that the eigenfunctions $f_l(\theta)$ are orthonormal as well as the reciprocity identity[16]

$$A(\theta+\pi,\alpha+\pi)=A(\alpha,\theta). \tag{30}$$

The solution is

$$Q_{lm}=\frac{k^2}{8\pi^2}\int\int|\sin(\theta-\alpha)|A(\theta,\alpha)f_l^*(\theta)f_m(\alpha)d\alpha\,d\theta. \tag{31}$$

Equations (25) and (31) specify a solution q_B to the linearized inverse problem. This solution is, in general, complex, even when the true potential q is purely real. A physical way to understand why the Born approximation yields a complex scattering potential for a lossless medium is to recognize that this approximation neglects multiple scattering and thus, the resulting output energy differs from the input energy. The corresponding scattering operator is then no longer unitary, and is only physically realizable by a potential with a nonzero imaginary part. For weak scattering, the energy discrepancy is small and so is the imaginary part of the potential.

The analytic solution of Eqs. (25) and (31) is equivalent to the well-known filtered backpropagation formula[13–15] and has the advantage of computational simplicity, as discussed later in this paper. Equivalence between the two formulas is shown by formulating an expansion of $e^{-ik\boldsymbol{\alpha}\cdot\mathbf{x}}$, viewed as a function of α, in terms of the orthonormal basis $\{f_m(\alpha)\}$. In view of Eqs. (11), this expansion yields the identity

$$e^{-ik\boldsymbol{\alpha}\cdot\mathbf{x}}=\sum_m E_m^*(\mathbf{x})f_m(\alpha). \tag{32}$$

Substituting Eq. (31) in Eq. (25) and using Eq. (32) as well as its conjugate gives

$$q_B(\mathbf{x})=\frac{k^2}{8\pi^2}\int\int|\sin(\alpha-\theta)|A(\theta,\alpha)e^{ik\mathbf{x}\cdot(\boldsymbol{\theta}-\boldsymbol{\alpha})}d\alpha\,d\theta, \tag{33}$$

which is the standard filtered backpropagation formula. Equation (33) yields the low-pass-filtered version of the true potential q if multiple scattering effects are negligible. The correct nonlinear generalization of the linearized low-pass filtered solution q_B is the minimal L^2 (or weighted L^2) solution q_M, which is of a form specified by Eq. (22).

The inverse scattering method developed above can also be used with any orthonormal set of basis functions for $L^2[0,2\pi]$. For instance, reconstructions can be performed using eigenfunctions of A for axisymmetric objects rather than using the eigenfunctions associated with the measured A. In this case, the eigenfunctions take the form

$$f_m(\theta)=\frac{1}{\sqrt{2\pi}}e^{im\theta}, \quad m=0,\pm 1,\pm 2,\ldots\,. \tag{34}$$

The retransmitted fields E_m can be analytically evaluated to be

$$E_m(r,\phi)=\sqrt{2\pi}i^m e^{im\phi}J_m(kr), \tag{35}$$

and the coefficients Q_{lm} for the low-pass-filtered reconstruction of q are given by

$$Q_{lm}=\frac{k^2}{16\pi^3}\int\int|\sin(\theta-\alpha)|A(\theta,\alpha)e^{-il\theta}e^{im\alpha}d\alpha\,d\theta. \tag{36}$$

While the retransmitted fields specified by Eq. (35) are not ideally matched to nonaxisymmetric scattering media, they can be analytically evaluated and stored for use in fast reconstructions. Since these retransmitted fields are also unaffected by uncertainties in scattering measurements, they are suitable for reconstructions from data corrupted by noise.

Finally, use of the eigenfunction method beyond linear inversion is demonstrated by considering the case where the inhomogeneous-medium retransmitted fields F can be estimated from a first approximation to the scattering potential q. One approach in this case is to solve the full system of equations defined by Eq. (24); however, a more numerically efficient correction to the Born approximation can be obtained by invoking the localized nonlinear approximation introduced in Ref. 22 for electromagnetic scattering. This approximation follows from writing the Lippman–Schwinger equation [Eq. (1)] in the form

$$p(\mathbf{x},\alpha)=\Gamma(\mathbf{x})\left(e^{ik\boldsymbol{\alpha}\cdot\mathbf{x}}-\int (p(\mathbf{y},\alpha)-p(\mathbf{x},\alpha))\right.$$

$$\left.\times q(\mathbf{y})G_0(\mathbf{x}-\mathbf{y})dy\right), \tag{37}$$

where the quantity $\Gamma(\mathbf{x})$, called the depolarization tensor in electromagnetic scattering,[22] is defined by

$$\Gamma(\mathbf{x})=\left(1+\int q(\mathbf{y})G_0(\mathbf{x}-\mathbf{y})dy\right)^{-1}. \tag{38}$$

The second term in Eq. (37) is presumed to be small because the singularity of the Green's function is cancelled by the difference term appearing in the integrand. Thus the total pressure may be approximated by the formula

$$p(\mathbf{x},\alpha)\approx\Gamma(\mathbf{x})e^{ik\boldsymbol{\alpha}\cdot\mathbf{x}}. \tag{39}$$

The form for the scattering potential given by Eq. (22) then becomes

$$q_M(\mathbf{x})\approx\frac{\Gamma(\mathbf{x})^2}{W(\mathbf{x})}\sum_l\sum_m Q_{lm}E_l(\mathbf{x})E_m^*(\mathbf{x}). \tag{40}$$

Substituting this form into Eq. (5) and using Eq. (39) gives

$$A(\theta,\alpha)\approx\sum_l\sum_m Q_{lm}\int e^{-ik\boldsymbol{\theta}\cdot\mathbf{x}}W(\mathbf{x})^{-1}E_l(\mathbf{x})E_m^*(\mathbf{x})$$

$$\times\Gamma(\mathbf{x})^3e^{ik\boldsymbol{\alpha}\cdot\mathbf{x}}\,dx. \tag{41}$$

An approximate nonlinear formula for the scattering potential q can be obtained by taking $W(\mathbf{x})\equiv\Gamma(\mathbf{x})^3$. Equation (41) then yields the coefficients Q_{lm} from Eq. (31) and the resulting solution for the scattering potential is

$$q_M(\mathbf{x})\approx\sum_l\sum_m Q_{lm}\frac{E_l(\mathbf{x})E_m^*(\mathbf{x})}{\Gamma(\mathbf{x})}. \tag{42}$$

The solution of Eq. (42) is simplified by making the further approximation

$$\frac{1}{\Gamma(\mathbf{x})}\approx 2-\Gamma(\mathbf{x}), \tag{43}$$

which is valid for small scattering potentials. This substitution results in

$$q_M(\mathbf{x})\approx\sum_l\sum_m Q_{lm}(2E_l(\mathbf{x})-F_l(\mathbf{x}))E_m^*(\mathbf{x}). \tag{44}$$

This nonlinear equation for the potential q_M can be approximately solved by using a form of the retransmitted field $F_l(\mathbf{x})$ corresponding to the low-pass-filtered potential q_B or to another estimate of the scattering potential.

II. COMPUTATIONAL METHODS

The focusing and imaging methods outlined in Sec. I were implemented using numerically computed scattered fields of inhomogeneous objects. Scattering operators were calculated using a method due to Kirsch and Monk,[23] in which an inner solution of the Helmholtz equation for a medium of variable sound speed is matched to an outer solution of integral equations that implicitly satisfy the Sommerfeld radiation condition. The inner solution is obtained using a finite-element method, while the outer integral equations are solved using Nyström's method.[23]

Scattering data were calculated numerically for a number of incident plane waves evenly distributed over M angles between 0 and 2π. For each incident-wave angle, the scattered field was computed at M far-field receiver angles between 0 and 2π, so that the angular sampling rate was $M/(2\pi)$ samples per radian. The number of receiver angles M should be chosen such that the scattered field has no significant frequency components above the Nyquist frequency of $M/(4\pi)$ samples per radian. This computation yields a discrete representation of the scattering operator A as an $M\times M$ matrix, A_M.

The eigenfunctions of A and their associated eigenvalues were estimated numerically by direct computation of the eigenvectors and eigenvalues of A_M. Retransmitted fields of eigenfunctions were evaluated numerically by numerical integration of Eq. (11). Images of inhomogeneous objects were then obtained using a straightforward numerical implementation of Eqs. (25) and (31). The integrals appearing in these equations were evaluated using corresponding discrete summations of the components of A_M and its eigenvectors. For comparison, standard diffraction tomography inversions were also performed by numerical integration of Eq. (33).

Stability of the eigenfunction imaging method was tested by inversion of noisy data obtained by adding numerically generated Gaussian white noise to the scattering matrix A_M. The rms amplitude of the noise was specified as a fraction of the rms value of A_M. Thus, for instance, a signal-to-noise ratio of 6 dB was obtained by adding noise with an rms amplitude one-half the rms value of A_M.

Inversions were also performed using the basis of eigenfunctions corresponding to axisymmetric inhomogeneities. In this case, the formula of Eq. (25) was implemented numerically using the trigonometric basis functions defined in Eq. (34), the retransmitted fields given in closed form in Eq. (35), and the coefficients defined in Eq. (36).

Nonlinear eigenfunction images were obtained using the analytic formula of Eq. (44) with the total pressure $p(\mathbf{x},\alpha)$ approximated by the total pressure for a medium including a cylinder of specified radius and compressibility contrast. This computation employed an exact solution for the scattering of a plane wave by a cylinder.[17]

III. NUMERICAL RESULTS

Focusing of eigenfunctions on a distributed scattering object is illustrated in Fig. 2. Here, the magnitudes of the retransmitted fields $E_1(\mathbf{x})$ and $E_2(\mathbf{x})$ are shown for an inhomogeneity consisting of a weakly scattering triangle ($\gamma_\kappa=0.01$) approximately two wavelengths in height. The triangle is shown in outline together with the retransmitted fields. The corresponding scattering operator, calculated using the finite-element/Nyström method described above, was represented by a matrix of size 128×128. The retransmitted fields show that the significant eigenfunctions of A specify incident-wave patterns that concentrate energy within the support of the inhomogeneity. Notable is that this focused energy is distributed throughout the support of the triangle.

Implementation of the eigenfunction method in focusing on pointlike scatterers is illustrated in Figs. 3 and 4. These figures, obtained using the linearized eigenfunction method, show not only diffraction-limited focusing but also quantitative reconstructions of the associated scattering potentials. Figure 3 shows images made from the scattered field of two pointlike scatterers at locations $(-0.5,0)$ and $(0,-0.2)$, each of radius 0.01 and compressibility variation -0.9. The numerically computed scattered field was sampled at 128 equally spaced angles for each of 128 incident-wave angles, so that the operator A was represented by a 128×128 matrix. The wave number used was 10, so that the scatterers were separated by approximately one wavelength. Since, in this case, two eigenvalues of A were much larger than the remaining eigenvalues, the basic reconstruction required only the use of two retransmitted fields. This result illustrates that, for an inhomogeneity consisting of finitely many pointlike scatterers, the present inverse scattering method provides an accurate reconstruction with diffraction-limited point resolution using a corresponding number of eigenfunctions.

A stability test of the eigenfunction method is illustrated in Fig. 4. This image shows a reconstruction of the two pointlike scatterers of Fig. 3 using the same scattering data with added Gaussian white noise for a signal-to-noise ratio of 3 dB. The method of reconstruction was identical to that used for Fig. 3. The reconstruction shown is almost indistinguishable from the noiseless reconstruction, indicating the stability of the eigenfunction imaging method.

Linear eigenfunction images of the triangular inhomogeneity of Fig. 2 are presented in Fig. 5. These images were constructed using the same scattering data as that used for Fig. 2. The first image, obtained using five retransmitted fields, shows that strong focusing is achieved using only a few eigenfunctions of A. The entire inhomogeneity is wellinsonified and little incident energy is transmitted outside the support of the inhomogeneity. The second image, obtained using 15 eigenfunctions, shows that the eigenfunction method rapidly converges to the ideal low-pass-filtered solution for the scattering potential. Notable is that the eigenfunction method using 15 eigenfunctions required 69.1 s of CPU time on a Sun SPARCstation 10, while an analogous image obtained using the diffraction tomography formula of Eq. (33), with the integrals evaluated in an analogous manner, required 3014.3 s.

Eigenfunction reconstructions of a test phantom, shown in Figs. 6–8, illustrate application of the eigenfunction imaging method to a larger-scale imaging problem. The phantom, also represented in Fig. 1, is a cylinder of compressibility contrast 0.01 and diameter of 5 mm. Internal objects include a water-filled (cystic) region of diameter 1 mm, a wire of diameter 0.1 mm and compressibility contrast -0.5, and an internal cylinder of diameter 1 mm and compressibility contrast -0.01. Scattered fields were calculated using the methods described above, with the operator A discretized as a matrix of 256×256 points. The first image shown in Fig. 6, obtained using the single wave number $k=10$ has high resolution but contains ringing (Gibbs phenomenon) artifacts and loss of contrast in the cystic region. These artifacts are removed by compounding of images obtained using five linearly spaced wave numbers, $8\leqslant k\leqslant12$, so that the dimensionless parameter ka varied between 20 and 30. The five-frequency image, shown in the second panel of Fig. 6, also shows increased point and contrast resolution compared to the single-frequency image. Both images shown in Fig. 6 were obtained using the linearized eigenfunction method described above, with 64 eigenfunctions of A for $k=8$, 9, and 10, 68 eigenfunctions for $k=11$, and 72 eigenfunctions for $k=12$.

Reconstructions of the test phantom obtained from noisy data are shown in Fig. 7. Gaussian white noise was added to the scattering data employed in Fig. 6, so that the signal-to-noise ratio was 6 dB at each of the frequencies employed. The reconstructions employed the formula of Eq. (25) and coefficients obtained from Eqs. (34)–(36). The numbers of basis functions employed were equal to the number of eigenfunctions employed in Fig. 6. These results indicate the stability of the method for large objects with scattering data severely degraded by noise.

Nonlinear reconstructions of the same test phantom, obtained using Eq. (44), are presented in Fig. 8 together with linear reconstructions. In the nonlinear reconstructions, the retransmitted fields $F_l(\mathbf{x})$ were estimated using pressure fields associated with a cylinder of diameter 5 mm and compressibility contrast 0.01.[17] The scattering data employed was identical to that used in Fig. 6(b), with five linearly spaced wave numbers such that $20\leqslant ka\leqslant30$. The number of eigenfunctions employed in each image were also the same as those used for the images in Fig. 6. The first panel shows the real part of the nonlinear reconstruction, taken along the line $y=0$, together with the real part of the analogous linear reconstruction from Fig. 6(b). The nonlinear reconstruction shows improved resolution over the linear reconstruction by increased height of the peak associated with the internal wire. The second panel shows the imaginary part of the nonlinear reconstruction with the corresponding linear reconstruction from Fig. 6(b). Here, the inaccuracy of the Born approximation results in a significant imaginary part for the linear reconstruction, while the true potential is purely real. The nonlinear inversion shows improved quantitative accuracy over the linear inversion by reduction of the reconstructed imaginary part.

IV. DISCUSSION

Our method has shown that eigenfunctions of the scattering operator can be employed to focus on distributed inhomogeneities as well as pointlike scatterers. However, the focusing on distributed inhomogeneities occurs in a different manner from focusing on pointlike scatterers. That is, the incident energy is not maximized at a single point within the medium. Instead, when combined according to the present reconstruction method, retransmitted eigenfunctions specify incident-wave distributions that distribute energy throughout the inhomogeneous region. This type of focusing, which results from the eigenfunction property of maximizing the scattered energy, is clearly connected to imaging of the medium by inverse scattering.

The quantitative inverse scattering method presented in this paper can considerably simplify imaging computations.

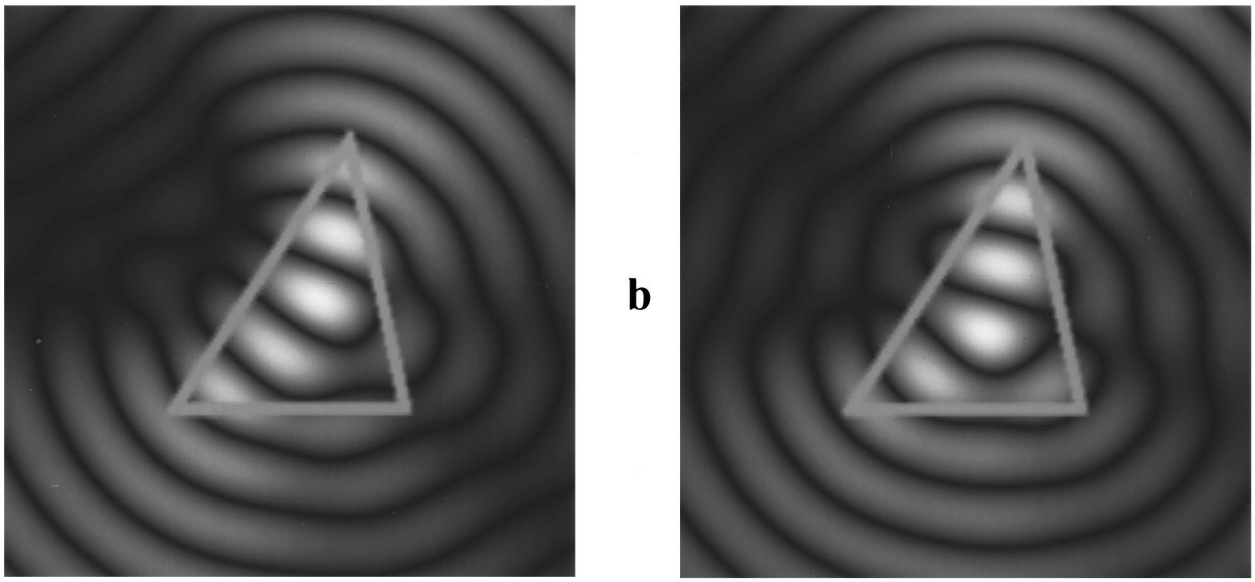

FIG. 2. Focusing on a distributed inhomogeneity. Magnitudes of the retransmitted fields of the two most significant eigenfunctions are shown on a linear gray scale with black indicating zero and white indicating maximum amplitude. The scattering object is a uniform triangle, compressibility contrast 0.01, within the sketched boundaries. (a) $E_1(\mathbf{x})$, (b) $E_2(\mathbf{x})$.

The computational complexity of the current method depends mainly on the number of significant eigenfunctions, which in turn depends only on the complexity of the scattering medium. Furthermore, the basis for expansion of the unknown medium is determined directly from the scattering data. Since the basis functions are closely related to the unknown medium, reconstructions performed using this basis employ a minimal amount of unnecessary information. This property gives the present inverse scattering method advantages over other methods in which a fixed basis is used to expand the unknown medium.[24–27] These advantages are most apparent for inhomogeneities a small number of wavelengths in size.

The present inverse scattering method also has the advantage of applicability to any medium for which the background pressure field can be estimated. Use of background pressure estimates can greatly improve accuracy over reconstructions based on simpler approximations. For instance, Born inversion can yield a spurious reconstructed imaginary part even when the true potential is real-valued; use of an estimated background pressure field can greatly reduce this error, as seen in Fig. 8. The inverse scattering method pre-

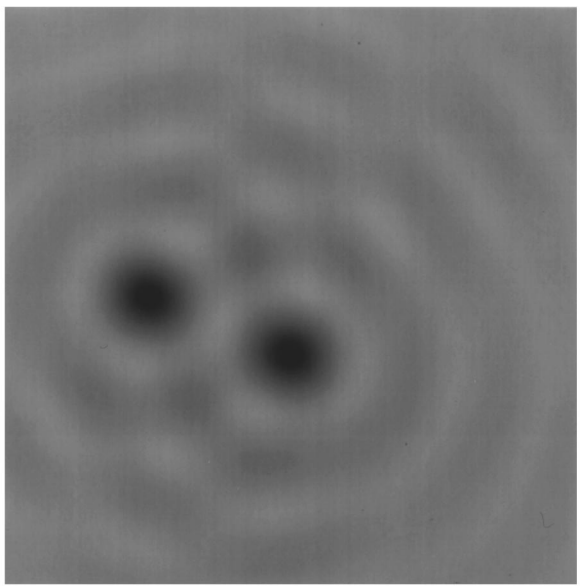

FIG. 3. Eigenfunction image of two pointlike scatterers, compressibility contrast -0.9, separated by approximately one wavelength. The image was obtained using retransmitted fields of the two most significant eigenfunctions.

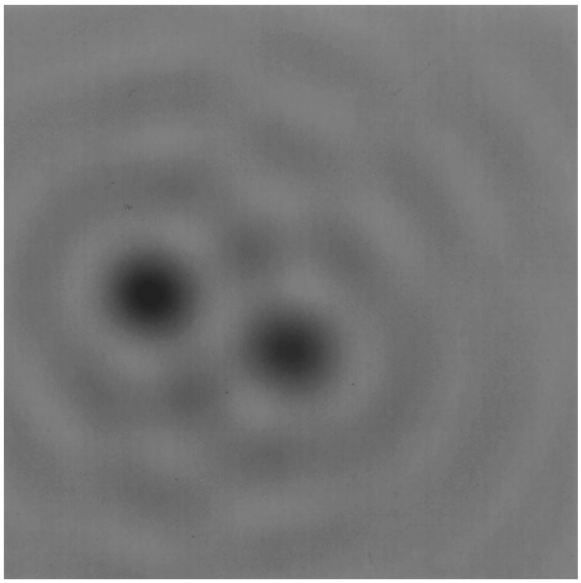

FIG. 4. Effect of noise on eigenfunction reconstruction. The object of Fig. 3 was reconstructed from two eigenfunctions of synthetically noised scattering data with a signal-to-noise ratio of 3 dB.

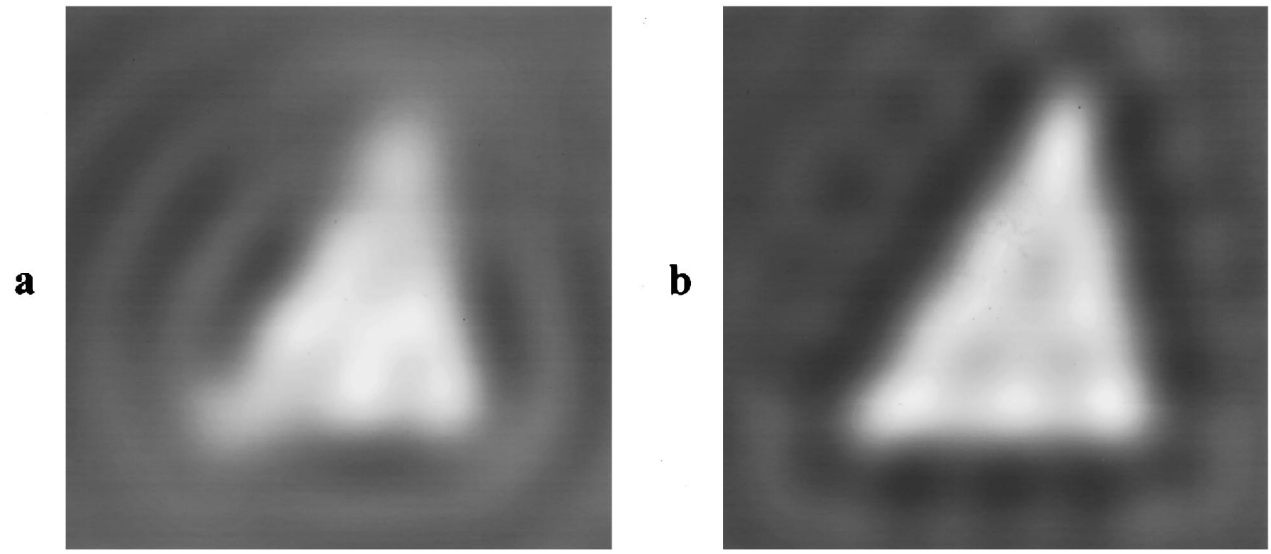

FIG. 5. Eigenfunction images of a triangle about three wavelengths in height having compressibility contrast 0.01. (a) Real part of an inversion obtained using retransmitted fields of five eigenfunctions. (b) Analogous image obtained using 15 eigenfunctions.

sented here is also extensible to any background medium for which a pressure field can be estimated, including moving fluids, layered or stratified media, and enclosed or otherwise bounded regions.

The imaging, focusing, and inverse scattering methods presented here also intrinsically take advantage of any potential increase in resolution that is associated with multiple scattering or other higher-order effects, as long as these effects are taken into account in the estimated pressure field. This increase in resolution is possible because the retransmitted fields of eigenfunctions may have desirable qualities, such as higher spatial-frequency components, that are associated with the presence of an inhomogeneous background. Such improvements in resolution have been shown experimentally for time-reversal focusing in a multiply scattering medium.[28]

The most significant eigenfunctions of A can be determined experimentally through iterative retransmission of received scattered fields in a manner similar to that performed in Refs. 1 and 10. This implementation of the power method[3] allows computation of the most significant eigenfunctions of A by analog means, which may be preferable to numerical computation for very large scattering objects. These eigenfunctions are useful as optimal incident-wave patterns for inverse scattering experiments.

The inverse scattering method presented here includes the assumption that the scattering potential is purely real, that is, the inhomogeneous medium is assumed to have zero absorption. Eigensystem analysis of the scattering operator A is more complicated in the presence of absorption.[29,30] However, the methods introduced here are expected to still

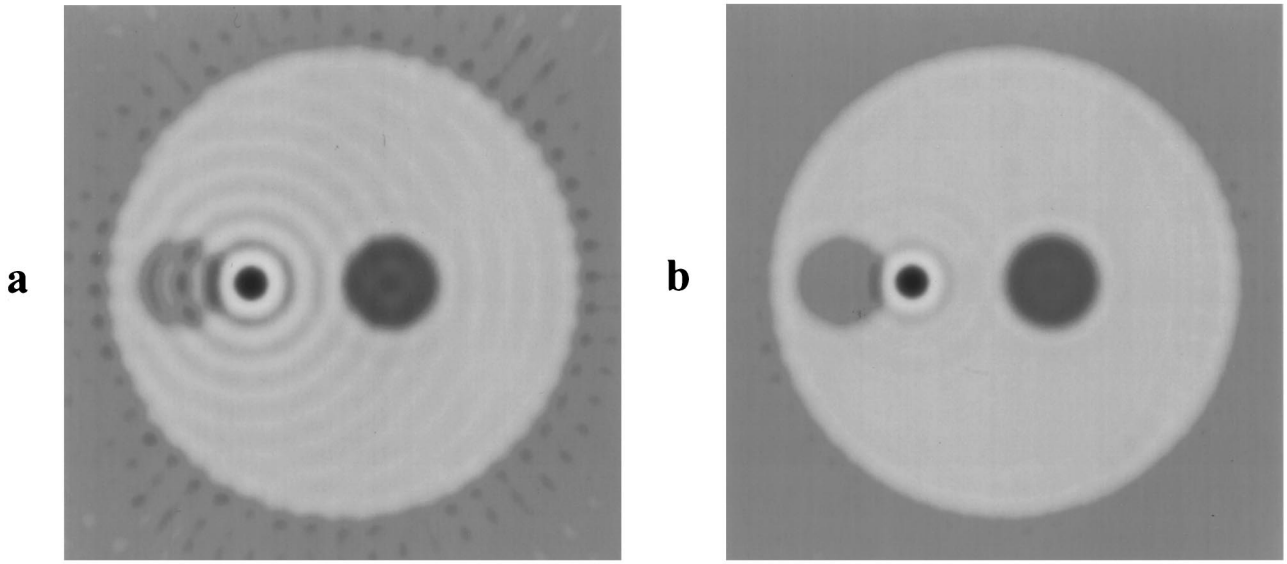

FIG. 6. Eigenfunction images of a test object having background compressibility contrast 0.01, a cystic (water-filled) region, a pointlike scatterer, and an internal cylinder. The images are shown on a logarithmic scale with a 40 dB dynamic range. (a) Real part of inversion obtained for a wave number such that $ka=25$. (b) Analogous image obtained using five wavenumbers such that $20<ka<30$.

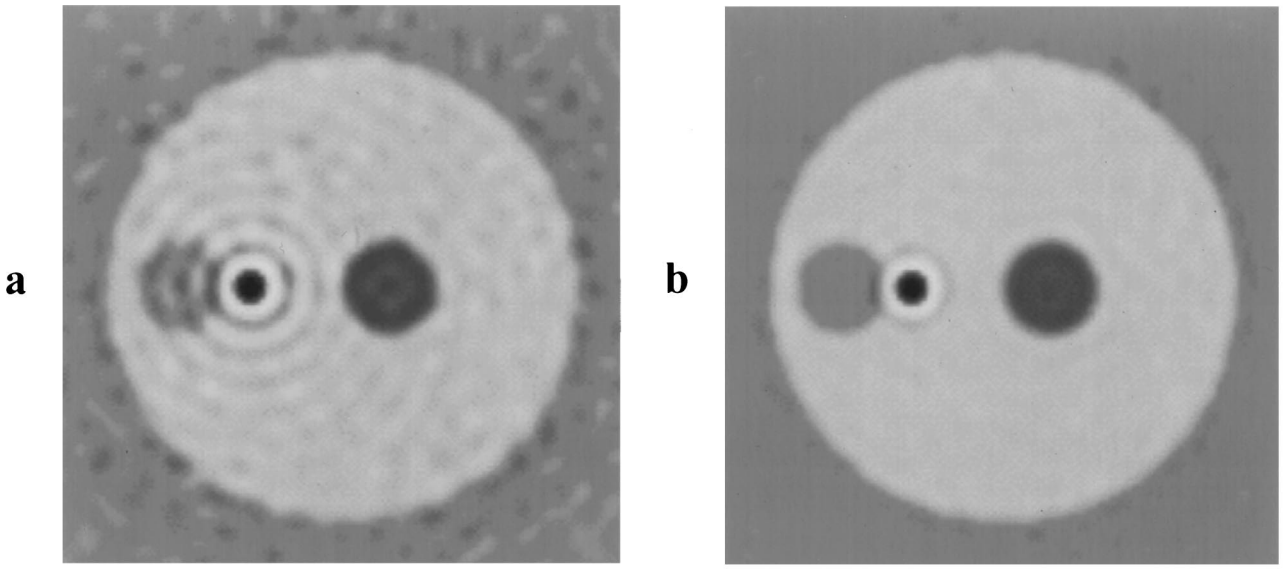

FIG. 7. Images of test object obtained using noised data with 6 dB signal-to-noise ratio. The images are shown on a logarithmic scale with a 40 dB dynamic range. (a) Real part of inversion obtained for a wave number such that $ka=25$. (b) Analogous image obtained using five wave numbers such that $20<ka<30$.

be useful for media such as biological tissue when absorption is finite but small.

A disadvantage of the inverse scattering method as currently implemented is that nonlinear inversion requires an accurate specification of the background acoustic field. This disadvantage is not unique to the eigenfunction method, but is a common feature of most current inversion methods. Recent theoretically exact methods, while not limited in this manner,[31,32] have not yet been implemented numerically.

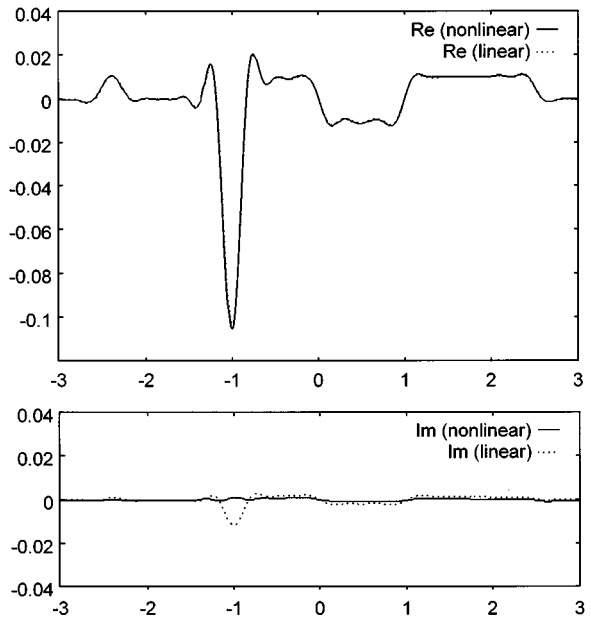

FIG. 8. Cross sections of real and imaginary parts of test object reconstructions using data from five wave numbers. Linear reconstructions were obtained using retransmitted fields in a homogeneous medium, while nonlinear reconstructions were obtained using retransmitted fields in a homogeneous medium and in a background cylinder of compressibility contrast 0.01. (a) Cross sections of real parts. (b) Cross sections of imaginary parts.

The general, nonlinear version of the eigenfunction imaging approach, as defined in Eqs. (24) and (44) and illustrated in Fig. 8, has obvious application to iterative reconstruction of unknown inhomogeneities. In such reconstructions, the total pressure field can be estimated at each iteration from a numerical solution of the direct scattering problem for the currently estimated inhomogeneity, and an eigenfunction inversion can be performed using this pressure field. This procedure can then be repeated to obtain improved estimates of the scattering potential until convergence is achieved.

V. CONCLUSION

A method for focusing and imaging using scattered fields has been presented. The method outlined here makes use of the physical properties of scattering operators by using their eigenfunctions as incident-wave patterns. The eigenfunctions have been shown to provide optimal focusing on pointlike and distributed scattering objects.

The inverse scattering scheme presented exploits the focusing properties of eigenfunctions as well as recent analytic results to obtain a robust and efficient means of quantitatively reconstructing unknown scattering media. This new method has a complexity dependent only on the size and complexity of the scattering medium. Particular cases of the method provide improved implementations of eigenfunction focusing and filtered backpropagation. The method can be implemented for any background medium for which the total acoustic pressure field can be estimated.

Another particular case of the presented method results in a nonlinear inverse scattering formula that yields a solution for the scattering potential q in terms of retransmitted fields of eigenfunctions in the scattering medium and in the background medium. This formula has been demonstrated to yield improvement in accuracy and resolution over Born inversion.

The ideas reported here are expected to be useful in further studies of inverse scattering, adaptive focusing, and ultrasonic imaging. The eigenfunctions of the scattering operator A, whether determined by iterative retransmission or by numerical diagonalization, may be used to focus through inhomogeneous media and to determine optimal incident-wave patterns for inverse scattering experiments. Also, the products of fields of eigenfunctions are expected to form a useful basis for expansion of unknown scattering media in iterative reconstruction algorithms.

ACKNOWLEDGMENTS

The authors thank Peter Monk for releasing his scattering problem solver under the Gnu General Public License and for assistance in the use of his code. Helpful discussions with Dong-Lai Liu, Petri Ola, and Fadil Santosa are acknowledged with pleasure. Funding for this work was provided by the F. V. Hunt Fellowship of the Acoustical Society of America, U.S. Army Grant No. DAMD17-94-J-4384, the University of Rochester Diagnostic Ultrasound Research Laboratory Industrial Associates, NIH Grants No. DK 45533 and No. HL 150855, and ONR Grant No. N00014-91-1107.

[1] D. Isaacson, ''Distinguishability of conductivities by electric current computed tomography,'' IEEE Trans. Med. Imaging **MI-5**, 91–95 (1986).
[2] D. G. Gisser, D. Isaacson, and J. C. Newell, ''Electric current computed tomography and eigenvalues,'' SIAM (Soc. Ind. Appl. Math.) J. Appl. Math. **50**, 1623–1634 (1990).
[3] E. Isaacson and H. S. Keller, *Analysis of Numerical Methods* (Wiley, New York, 1966), pp. 147–159.
[4] G. S. Agarwal, A. T. Friberg, and E. Wolf, ''Scattering theory of distortion correction by phase conjugation,'' J. Opt. Soc. Am. **73**, 529–538 (1983).
[5] R. Mittra and T. M. Habashy, ''Theory of wave-front distortion by phase conjugation,'' J. Opt. Soc. Am. A **1**, 1103–1109 (1984).
[6] O. Ikeda, ''An image reconstruction algorithm using phase conjugation for diffraction-limited imaging in an inhomogeneous medium,'' J. Acoust. Soc. Am. **85**, 1602–1606 (1989).
[7] D. R. Jackson and D. R. Dowling, ''Phase conjugation in underwater acoustics,'' J. Acoust. Soc. Am. **89**, 171–181 (1991).
[8] M. Fink, ''Time-reversal of ultrasonic fields—Part I: Basic principles,'' IEEE Trans. Ultrason. Ferroelectr. Freq. Control **39**, 555–567 (1992).
[9] D. Cassereau and M. Fink, ''Time-reversal of ultrasonic fields—Part III: Theory of the closed time-reversal cavity,'' IEEE Trans. Ultrason. Ferroelectr. Freq. Control **39**, 579–592 (1992).
[10] C. Prada, J. -L. Thomas, and M. Fink, ''The iterative time-reversal process: analysis of the convergence,'' J. Acoust. Soc. Am. **97**, 62–71 (1995).
[11] C. Prada, S. Manneville, D. Spoliansky, and M. Fink, ''Decomposition of the time reversal operator: Detection and selective focusing on two scatterers,'' J. Acoust. Soc. Am. **99**, 2067–2076 (1996).
[12] K. Chadan and P. C. Sabatier, *Inverse Problems in Quantum Scattering Theory* (Springer-Verlag, New York, 1989).
[13] A. J. Devaney, ''A filtered backpropagation algorithm for diffraction tomography,'' Ultrason. Imaging **4**, 336–350 (1982).
[14] A. J. Devaney and G. Beylkin, ''Diffraction tomography using arbitrary transmitter and receiver surfaces,'' Ultrason. Imaging **6**, 181–193 (1984).
[15] A. Witten, J. Tuggle, and R. C. Waag, ''A practical approach to ultrasonic imaging using diffraction tomography,'' J. Acoust. Soc. Am. **83**, 1645–1652 (1988).
[16] J. R. Taylor, *Scattering Theory* (Wiley, New York, 1972).
[17] P. M. Morse and K. U. Ingard, *Theoretical Acoustics* (McGraw-Hill, New York, 1968), Chap. 8.
[18] P. M. Morse and H. Feshbach, *Methods of Theoretical Physics* (McGraw-Hill, New York, 1953), Vol. I.
[19] M. Reed and B. Simon, *Methods of Mathematical Physics* (Academic, San Diego, 1980), Vol. III.
[20] G. N. Watson, *A Treatise on the Theory of Bessel Functions* (Macmillan, New York, 1944), 2nd ed., p. 359.
[21] D. C. Dobson and F. Santosa, ''Resolution and stability analysis of an inverse problem in electrical impedance tomography: dependence on the input current patterns,'' SIAM (Soc. Ind. Appl. Math.) J. Appl. Math. **54**, 1542–1560 (1994).
[22] T. M. Habashy, R. W. Groom, and B. R. Spies, ''Beyond the Born and Rytov approximations: a nonlinear approach to electromagnetic scattering,'' J. Geophys. Res. **98**, 1759–1775 (1993).
[23] A. Kirsch and P. Monk, ''An analysis of the coupling of finite element and Nyström methods in acoustic scattering,'' IMA J. Num. Anal. **14**, 523–544 (1994).
[24] T. J. Cavicchi and W. D. O'Brien, ''Numerical study of higher-order diffraction tomography via the sinc basis moment method,'' Ultrason. Imaging **11**, 42–74 (1989).
[25] D. T. Borup, S. A. Johnson, W. W. Kim, and M. J. Berggren, ''Nonperturbative diffraction tomography via Gauss-Newton iteration applied to the scattering integral equation,'' Ultrason. Imaging **14**, 69–85 (1992).
[26] W. C. Chew and G. P. Otto, ''Microwave imaging of multiple conducting cylinders using local shape functions,'' IEEE Microwave Guided Wave Lett. **2**, 284–286 (1992).
[27] H. Gan, R. Ludwig, and P. L. Levin, ''Nonlinear diffractive inverse scattering for multiple scattering in inhomogeneous acoustic background media,'' J. Acoust. Soc. Am. **97**, 764–776 (1995).
[28] A. Derode, P. Roux, and M. Fink, ''Acoustic time-reversal through high-order multiple scattering,'' *1995 IEEE Ultrasonics Symposium Proceedings* (IEEE, Piscataway, NJ, 1995), Vol. 2, pp. 1091–1094.
[29] D. Colton and R. Kress, ''Eigenvalues of the far field operator and inverse scattering theory,'' SIAM J. Math. Anal. **26**, 601–615 (1995). One of the anonymous reviewers is thanked for drawing the authors' attention to Refs. 29 and 30.
[30] D. Colton and R. Kress, ''Eigenvalues of the far field operator for the Helmholtz equation in an absorbing medium,'' SIAM (Soc. Ind. Appl. Math.) J. Appl. Math. **55**, 1724–1735 (1995).
[31] A. I. Nachman, ''Reconstructions from boundary measurements,'' Ann. Math. **128**, 531–576 (1988).
[32] A. I. Nachman, ''Global uniqueness for a two-dimensional inverse boundary problem,'' Ann. Math. **143**, 71–96 (1996).